DOI: 10.1002/ejic.200700810

Novel (3,4)- and (4,5)-Connected Lanthanide Metal–Organic Frameworks

Xian-Wen Wang,*[a] Xing Li,[b] Jing-Zhong Chen,[a] Guang Zheng,*[c] and Han-Lie Hong[a]

Keywords: Mixed nodes / Lanthanides / Metal–organic frameworks

The three-dimensional lanthanide noninterpenetrating metal–organic frameworks formulated as [Ln(3,5-pdc)-$(C_2O_4)_{0.5}(H_2O)_2$]·H_2O (Ln = Lu^{III}, Gd^{III}, Tm^{III} and Yb^{III} for complex **1**–**4**, respectively; 3,5-pdc = 3,5-pyridinedicarboxylate) were synthesized by hydrothermal reactions of 3,5-H_2pdc with lanthanide oxide and perchloric acid. Compound **1** shows (3,4)-connected $(4.8^2)(4.8^5)$ dmc-type topological network, and complexes **2**–**4** display the novel (4,5)-connected $(4^4.6.8)(4^4.6^2.8^4)$ xww-type topology. The lanthanide-mediated transformation of CO_2 to oxalate under hydrothermal conditions was observed. The fluorescence properties of complexes **1**–**4** were investigated.
(© Wiley-VCH Verlag GmbH & Co. KGaA, 69451 Weinheim, Germany, 2008)

Introduction

Great interest has been focused on the rapidly expanding field of crystal engineering of higher dimensionality metal–organic frameworks (MOFs)[1] due to their intriguing network topologies as well as their potential application as functional materials in many areas such as separations and catalysis,[2] gas storage,[3] and magnetism.[4] Carboxylate groups display a variety of binding geometries, such as, monodentate terminal, chelating, bidentate bridging, and monodentate bridging, in coordination chemistry and the active sites of metalloenzymes.[5] A significant number of highly symmetric carboxylate bridged MOFs have been obtained and well characterized because of their fascinating structures of metal–carboxylate clusters, underlying applications, and novel topological networks.[6,7] Many higher dimensional MOFs represent themselves as realistic targets of inorganic compounds or minerals in nature based on highly symmetric building blocks with the basic connectivity of 3, 4, or 6 and topologies such as srs, ths, cds, nbo, dia, pts, pcu, and so on.[8,9] Recently, particular attention has been attracted to the use of unsymmetrical building blocks with different connectivities to generate unique topological nets. For example, nets containing both three- and four-connected nodes form such networks as (3,4)-connected characteristic tfa net, dmc net, boracite net, ReO_3, and Pt_3O_4, and other nets consisting of mix-connected nodes form such topologies as (3,6)-connected rutile net, (4,6)-connected α-Al_2O_3 net, and (4,8)-connected CaF_2 net.[8,10] However, only two examples of (3,4)-connected $(4.8^2)(4.8^5)$-dmc net are observed in the literature up to date: the inorganic compound Ag_2HgS_2 and the coordination compound $[H_2N(CH_2)_2NH_2]_{0.5}$·$ZnHPO_3$.[8c,8d,11] The (4,5)-connected topological net is scarcely described. The inorganic compound $ThCr_2Si_2$ exhibits the (4,5)-connected tcs net,[12a] and Batten described one hydrogen bonding extended metal–organic cluster compound displaying the (4,5)-connected interpenetrating topology.[12b] In this contribution, we present unique mixed-node topological nets of the (3,4)-connected $(4.8^2)(4.8^5)$ dmc-type and (4,5)-connected $(4^4.6.8)(4^4.6^2.8^4)$ topological noninterpenetrating porous metal–organic open frameworks constructed from lanthanide ions and 3,5-pdc and oxalate: [Ln(3,5-pdc)$(C_2O_4)_{0.5}$-$(H_2O)_2$]·H_2O (Ln = Lu^{III}, Gd^{III}, Tm^{III} and Yb^{III} for complex **1**–**4**, respectively; 3,5-pdc = 3,5-pyridinedicarboxylate).

Lanthanide ions possess fascinating coordination geometries and interesting luminescent and magnetic properties, and they can be used to construct unprecedentedly intriguing structures with special properties in material science. For example, they can serve as superconductors, magnetic materials, luminescence probes, or catalysts.[13] In contrast, the progress of the analogous chemistry towards lanthanide metals has been slow,[14] which may be attributed, at least partially, to the tendency of these ions to possess high coordination. This favors the formation of condensed structures, which makes it difficult to control the synthetic reactions. Although variety in the coordination sphere of lanthanide ions makes design difficult, this flexibility makes the f-block metal ions fascinating for the discovery of new and unusual network topologies.[14d]

[a] Faculty of Material Science and Chemical Engineering, China University of Geoscience,
Hubei, Wuhan 430074, China
E-mail: wxw10108092@yahoo.com.cn
[b] Faculty of Material Science and Chemical Engineering, Ningbo University, Zhejiang,
Ningbo 315211, China
E-mail: wxw10108092@yahoo.com.cn
[c] Maths and Physics Department, China University of Geoscience,
Hubei, Wuhan 430074, China
E-mail: gzheng25@yahoo.com
Supporting information for this article is available on the WWW under http://www.eurjic.org or from the author.

© 2008 Wiley-VCH Verlag GmbH & Co. KGaA, Weinheim

Results and Discussion

Preparation of the Complexes

We carried out the reactions of 3,5-pyridinedicarboxylatic acid with lanthanide oxides, perchloric acid, and $Mn(ClO_4)_2$ under hydrothermal conditions to synthesize 3d–4f species, and we isolated a small quantity of crystalline products. Single-crystal X-ray analyses and ICP experimental results indicate that all the complexes consist of only Ln^{III} ions, 3,5-pdc anionic ligands, and unexpected oxalate ligands. The reaction of 3,5-H_2pdc with lanthanide oxides and perchloric acid in the absence of $Mn(ClO_4)_2$ under the same hydrothermal conditions resulted in the successful isolation of $[Ln(3,5\text{-pdc})(C_2O_4)_{0.5}(H_2O)_2]\cdot H_2O$ (Ln = Lu^{III}, Gd^{III}, Tm^{III}, and Yb^{III} for complex **1**–**4**, respectively) and the previously reported $[Ln(3,5\text{-pdc})(C_2O_4)_{0.5}(H_2O)_2]\cdot H_2O$ (Ln = Dy^{III}, Sm^{III}, Ho^{III}, Eu^{III}, La^{III}, Nd^{III}, and Er^{III} for complex **5**–**11**) complexes. The transformations of CO_2 to oxalate have been reported through chemical, photochemical, and electrochemical syntheses.[15a–15d] Recently, the lanthanide-mediated in situ transformation of CO_2 to an oxalate ligand under hydrothermal conditions has been observed.[15e–15g] Although the origin of the reductive coupling remains unclear, one possibility is that the oxalate ligands result from the coupling of CO_2 molecules released from the H_2pdc ligands (Scheme 1).[15f–15i]

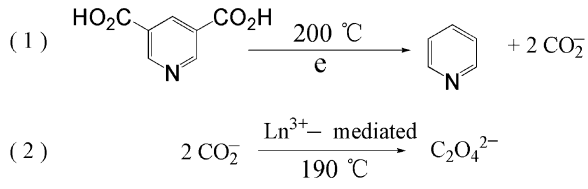

Scheme 1.

Description of the Crystal Structures

Although all the complexes have a common chemical formula and they all pertain to the monoclinic system, compound **1** crystallizes in the $P2_1/c$ space group and compounds **2**–**4** crystallize in the $P2_1/n$ space group. In addition to the structural data of **1**, we will describe only the structure of **2** in detail because complexes **2**–**4** are isostructural. Tables 1 and 2 give selected bond lengths and angles for **1**–**4**, whereas Table 3 summarizes the important crystal data for **1**–**4**.

[Lu(3,5-pdc)(C_2O_4)$_{0.5}$(H_2O)$_2$]·H_2O (1)

The asymmetric unit of compound **1** contains one Lu^{III} atom, one 3,5-pdc ligand, one-half of an oxalate group, two coordinated water molecules, and one lattice aqua. As shown in Figure 1, the Lu^{III} atom is surrounded by eight O atoms, of which two come from the coordinated water molecules, two come from one oxalate group, and the rest come from three 3,5-pdc ligands; the eight-coordinate Lu^{III} atom adopts a square antiprism geometry. The Lu–O bond

Table 1. The selected bond lengths (Å) and angles (°) for **1** and **2**.[a]

1					
Lu1–O2	2.241(4)	O2–Lu1–O1$^{\#1}$	77.99(15)	O7–Lu1–O6$^{\#3}$	77.27(14)
Lu1–O1$^{\#1}$	2.259(4)	O2–Lu1–O7	74.16(14)	O3$^{\#2}$–Lu1–O6$^{\#3}$	128.05(13)
Lu1–O7	2.292(4)	O1$^{\#1}$–Lu1–O7	86.57(14)	O8–Lu1–O6$^{\#3}$	74.36(13)
Lu1–O3$^{\#2}$	2.300(4)	O2–Lu1–O3$^{\#2}$	80.30(14)	O2–Lu1–O5	143.11(15)
Lu1–O8	2.312(4)	O1$^{\#1}$–Lu1–O3$^{\#2}$	79.33(14)	O1$^{\#1}$–Lu1–O5	70.46(13)
Lu1–O6$^{\#3}$	2.327(4)	O7–Lu1–O3$^{\#2}$	152.90(14)	O7–Lu1–O5	85.15(14)
Lu1–O5	2.347(4)	O2–Lu1–O8	76.54(15)	O3$^{\#2}$–Lu1–O5	111.17(14)
Lu1–O4$^{\#2}$	2.447(4)	O1$^{\#1}$–Lu1–O8	147.98(13)	O8–Lu1–O5	139.24(13)
O3$^{\#2}$–Lu1–O4$^{\#2}$	55.05(13)	O7–Lu1–O8	104.65(14)	O6$^{\#3}$–Lu1–O5	69.39(13)
O8–Lu1–O4$^{\#2}$	78.24(15)	O3$^{\#2}$–Lu1–O8	77.53(13)	O2–Lu1–O4$^{\#2}$	132.37(14)
O6$^{\#3}$–Lu1–O4$^{\#2}$	76.83(14)	O2–Lu1–O6$^{\#3}$	131.94(14)	O1$^{\#1}$–Lu1–O4$^{\#2}$	105.82(15)
O5–Lu1–O4$^{\#2}$	75.98(14)	O1$^{\#1}$–Lu1–O6$^{\#3}$	137.66(14)	O7–Lu1–O4$^{\#2}$	152.01(13)
2					
Gd1–O3	2.3095(15)	O3–Gd1–O4$^{\#1}$	101.29(6)	O2$^{\#2}$–Gd1–O5	71.34(6)
Gd1–O4$^{\#1}$	2.3115(16)	O3–Gd1–O2$^{\#2}$	88.71(6)	O1$^{\#3}$–Gd1–O5	75.50(5)
Gd1–O2$^{\#2}$	2.3356(16)	O4$^{\#1}$–Gd1–O2$^{\#2}$	149.92(6)	O3–Gd1–O7	68.64(6)
Gd1–O1$^{\#3}$	2.3678(15)	O3–Gd1–O1$^{\#3}$	149.27(5)	O4$^{\#1}$–Gd1–O7	75.77(6)
Gd1–O5	2.4422(16)	O4$^{\#1}$–Gd1–O1$^{\#3}$	84.11(6)	O2$^{\#2}$–Gd1–O7	81.84(6)
Gd1–O7	2.4642(17)	O2$^{\#2}$–Gd1–O1$^{\#3}$	101.71(6)	O1$^{\#3}$–Gd1–O7	141.01(5)
Gd1–O8	2.4658(16)	O3–Gd1–O5	80.80(6)	O5–Gd1–O7	139.57(5)
Gd1–O6$^{\#4}$	2.4772(16)	O4$^{\#1}$–Gd1–O5	137.94(6)	O3–Gd1–O8	138.22(6)
O4$^{\#1}$–Gd1–O8	78.25(6)	O7–Gd1–O8	70.91(6)	O1$^{\#3}$–Gd1–O6$^{\#4}$	78.04(5)
O2$^{\#2}$–Gd1–O8	75.58(6)	O3–Gd1–O6$^{\#4}$	74.54(5)	O5–Gd1–O6$^{\#4}$	65.91(6)
O1$^{\#3}$–Gd1–O8	72.50(5)	O4$^{\#1}$–Gd1–O6$^{\#4}$	74.15(5)	O7–Gd1–O6$^{\#4}$	125.87(6)
O5–Gd1–O8	127.32(6)	O2$^{\#2}$–Gd1–O6$^{\#4}$	135.89(5)	O8–Gd1–O6$^{\#4}$	141.25(5)

[a] Symmetry transformations used to generate equivalent atoms are as follows: **1**: #1 = x, –y + 3/2, z + 1/2; #2 =- x, –y + 2, –z + 1; #3 = –x + 1, –y + 2, –z + 2; #4 = x, –y + 3/2, z – 1/2. **2**: #1 = –x, –y + 2, –z + 1; #2 = –x + 1/2, y – 1/2, –z + 1/2; #3 = x, y – 1, z; #4 = –x + 1, –y + 2, –z + 1; #5 = x, y + 1, z.

 © 2008 Wiley-VCH Verlag GmbH & Co. KGaA, Weinheim

Table 2. The selected bond lengths (Å) and angles (°) for **3** and **4**.[a]

3					
Tm1–O3$^{\#1}$	2.2521(19)	O3$^{\#1}$–Tm1–O4$^{\#2}$	100.84(7)	O2$^{\#3}$–Tm1–O5$^{\#4}$	70.92(7)
Tm1–O4$^{\#2}$	2.2569(19)	O3$^{\#1}$–Tm1–O2$^{\#3}$	87.91(7)	O1–Tm1–O5$^{\#4}$	75.48(7)
Tm1–O2$^{\#3}$	2.2956(19)	O4$^{\#2}$–Tm1–O2$^{\#3}$	149.97(7)	O3$^{\#1}$–Tm1–O8	137.92(8)
Tm1–O1	2.3128(19)	O3$^{\#1}$–Tm1–O1	149.57(7)	O4$^{\#2}$–Tm1–O8	78.59(7)
Tm1–O5$^{\#4}$	2.386(2)	O4$^{\#2}$–Tm1–O1	84.20(7)	O2$^{\#3}$–Tm1–O8	75.89(7)
Tm1–O8	2.404(2)	O2$^{\#3}$–Tm1–O1	102.72(7)	O1–Tm1–O8	72.50(7)
Tm1–O7	2.415(2)	O3$^{\#1}$–Tm1–O5$^{\#4}$	81.46(7)	O5$^{\#4}$–Tm1–O8	126.60(7)
Tm1–O6	2.442(2)	O4$^{\#2}$–Tm1–O5$^{\#4}$	138.49(7)	O3$^{\#1}$–Tm1–O7	68.85(8)
O4$^{\#2}$–Tm1–O7	75.74(8)	O8–Tm1–O7	70.36(8)	O1–Tm1–O6	78.45(7)
O2$^{\#3}$–Tm1–O7	80.96(7)	O3$^{\#1}$–Tm1–O6	74.41(7)	O5$^{\#4}$–Tm1–O6	67.16(7)
O1–Tm1–O7	140.47(7)	O4$^{\#2}$–Tm1–O6	73.57(7)	O8–Tm1–O6	141.36(7)
O5$^{\#4}$–Tm1–O7	139.62(7)	O2$^{\#3}$–Tm1–O6	136.29(7)	O7–Tm1–O6	125.75(7)
4					
Yb1–O3$^{\#1}$	2.240(3)	O4$^{\#2}$–Yb1–O1	84.25(11)	O4$^{\#2}$–Yb1–O7	78.76(11)
Yb1–O4$^{\#2}$	2.249(3)	O2$^{\#3}$–Yb1–O1	102.72(11)	O2$^{\#3}$–Yb1–O7	75.97(11)
Yb1–O2$^{\#3}$	2.287(3)	O3$^{\#1}$–Yb1–O6$^{\#4}$	81.65(12)	O1–Yb1–O7	72.08(9)
Yb1–O1	2.303(3)	O4$^{\#2}$–Yb1–O6$^{\#4}$	138.36(10)	O6$^{\#4}$–Yb1–O7	126.44(12)
Yb1–O6$^{\#4}$	2.389(4)	O2$^{\#3}$–Yb1–O6$^{\#4}$	70.98(11)	O8–Yb1–O7	70.30(10)
Yb1–O8	2.406(3)	O1–Yb1–O6$^{\#4}$	75.57(10)	O3$^{\#1}$–Yb1–O5	74.47(10)
Yb1–O7	2.407(3)	O3$^{\#1}$–Yb1–O8	68.86(11)	O4$^{\#2}$–Yb1–O5	73.52(10)
Yb1–O5	2.440(3)	O4$^{\#2}$–Yb1–O8	75.95(12)	O2$^{\#3}$–Yb1–O5	136.21(11)
O3$^{\#1}$–Yb1–O4$^{\#2}$	100.72(12)	O2$^{\#3}$–Yb1–O8	80.63(12)	O1–Yb1–O5	78.80(10)
O3$^{\#1}$–Yb1–O2$^{\#3}$	87.70(11)	O1–Yb1–O8	140.11(10)	O6$^{\#4}$–Yb1–O5	67.09(11)
O4$^{\#2}$–Yb1–O2$^{\#3}$	150.08(10)	O6$^{\#4}$–Yb1–O8	139.64(11)	O8–Yb1–O5	126.01(11)
O3$^{\#1}$–Yb1–O1	150.01(10)	O3$^{\#1}$–Yb1–O7	137.89(10)	O7–Yb1–O5	141.39(9)

[a] Symmetry transformations used to generate equivalent atoms are as follows. **3**: #1 = *x*, *y* – 1, *z*; #2 = –*x*, –*y* + 2, –*z* + 1; #3 = –*x* + 1/2, *y* – 1/2, –*z* + 1/2; #4 = –*x* + 1, –*y* + 1, –*z* + 1. **4**: #1 = *x*, *y* – 1, *z*; #2 = –*x*, –*y* + 1, –*z* + 1; #3 = –*x* + 1/2, *y* – 1/2, –*z* + 1/2; #4 = –*x* + 1, –*y*, –*z* + 1.

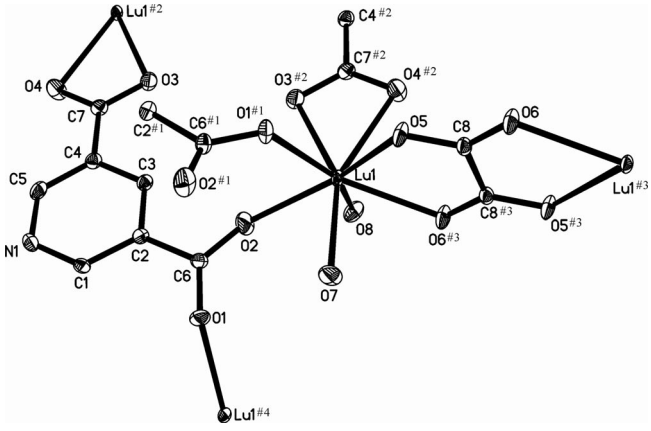

Figure 1. ORTEP drawing of the coordination environments around Lu ions in **1** with thermal ellipsoids at the 40% probability level. The isolated water molecules and H atoms are omitted for clarity.

lengths range from 2.246(1) to 2.447(4) Å, and they are similar to those found in other Lu^{III} complexes.[16] Noticeably, the pyridyl nitrogen atom of the 3,5-pdc ligand is absent in the coordination, and the 5-positioned carboxylate group coordinates in a bidentate chelating mode, whereas the 3-positioned carboxylate group coordinates in a *syn–syn* mode with the two oxygen atoms linking two distinct metal atoms, respectively. As a result, each of the 3,5-pdc ligands acts as a μ_3-bridge joining three metal atoms, and each of the metal atoms also joins three 3,5-pdc organic groups (Figure 2a). The Lu atoms are bridged by the 3,5-pdc ligands into two-dimensional sheets parallel to (100). Along the [001] direction, there exist π–π stacking interactions between the neighboring pyridyl rings and the contacting centroid distance is 3.494 Å (Figure 2a). The sheets are further bridged by the oxalate ligands into a 3D metal–organic framework, in which the lattice water molecules fill the channels along *c* axis (Figure 2b).

From a topological viewpoint, the sheets can be considered as the 3-connected subunits with a topology of 4.8^2 (Figure 2c). The oxalate ligands can be represented simply as links between the Lu nodes. Thus, from the above analysis, the network topology of **1** can be simplified by considering only the (3,4)-connected topology. Relative to the known (3,4)-connected nets such as the uniform nets (n,4^3) (n = 6–9) and other nonuniform (3,4)-connected nets, for example, the idealized structure of Ge_3N_4, a number of complex oxides (Be_2GeO_4, Be_2SiO_4, Zn_2SiO_4, Li_2MoO_4, and Li_2WO_4), and boracite,[9,17] the topology of **1** is novel because the 3- and 4-connected nodes do not alternate. The pdc and Lu act as 3- and 4-connected centers with the Schläfli symbol ($4;8^2$) and ($4;8^5$),[18] respectively. Thus, complex **1** shows a (3,4)-connected (4.8^2)(4.8^5) topological network (Figure 2d) with the vertex symbol or long symbol of ($4.8_3.8_3$)($4.8_2.8_2.8_3.8_2.8_3$) and coordination sequences of (3, 8, 17, 30, 48, 69, 90, 119, 157, 183, 725) for the 3-connected nodes and (4, 8, 18, 33, 47, 68, 95 120, 150, 191, 735) for the 4-connected nodes.[19] The inorganic compound Ag_2HgS_2 and coordination compound $[H_2N(CH_2)_2NH_2]_{0.5}$·

 © 2008 Wiley-VCH Verlag GmbH & Co. KGaA, Weinheim

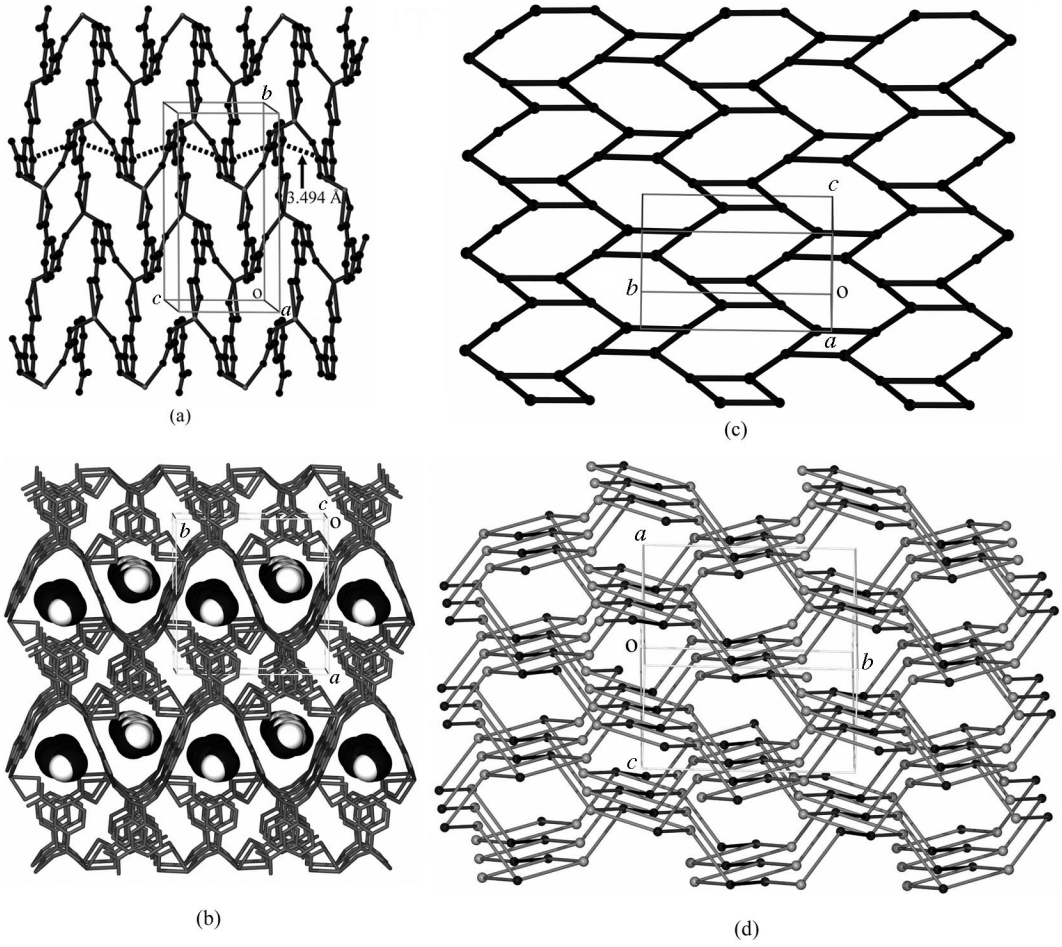

Figure 2. (a) The two-dimensional sheet parallel to (100) of **1** constructed by 3,5-pdc ligands and metal atoms (the dashed lines suggest π–π stacking interactions between the neighboring pyridyl rings); (b) 3D structure of **1**, showing the lattice water occupying the channels along the *c* axis; (c) 3-connected 4.8^2 subnet of **1**; (d) perspective view down from the *c* axis showing (3,4)-connected dmc topology for **1** (the gray spheres represent 3,5-pdc ligands; the black balls indicate Lu atoms, and the black solid lines are oxalate groups).

$ZnHPO_3$[11] also possess (3,4)-connected $(4.8^2)(4.8^5)$ topological networks; the topology was defined with a three-letter code of $(4.8^2)(4.8^5)$-"dmc" by Proserpio and O'Keeffe.[8c,8d,20]

Within the crystal structure, the channel water molecules accept hydrogen atoms (H7B) from the coordinated water molecules (O7) and donate hydrogen atoms (H1A) to carboxylate O4 atoms to form O7–H7B···O1w^{i} strong hydrogen bonding interactions and O1w–H1A···O4^{ii} weak hydrogen bonding interactions, respectively [*d*(O7···O1w^{i}) = 2.629(1) Å, ∠(O7–H7B···O1w^{i}) = 160°; *d*(O1w···O4^{ii}) = 3.237(1) Å, ∠(O1w–H1A···O4^{ii}) = 147.5°; symmetry codes i: *x*, *y*, 1 + *z*; ii: 1 + *x*, *y*, *z*]. The coordinated water molecules (O8) donate hydrogen atoms to oxalate O5 and the uncoordinated pyridyl nitrogen atoms to form O8–H8A···O5^{iii} and O8–H8B···N1^{iv} strong hydrogen bonding interactions, respectively [*d*(O8···O5^{iii}) = 2.846(5) Å, ∠(O8–H7A···O5^{iii}) = 145.83°; *d*(O8···N1^{iv}) = 2.883(6) Å, ∠(O8B–H1B···N1^{iv}) = 154.88°; symmetry codes iii: *x*, *y*, –1 + *z*; iv: 1 + *x*, *y*, *z*]. The hydrogen bonding interactions and the π–π stacking interactions play a key role to stabilize the crystal structure.

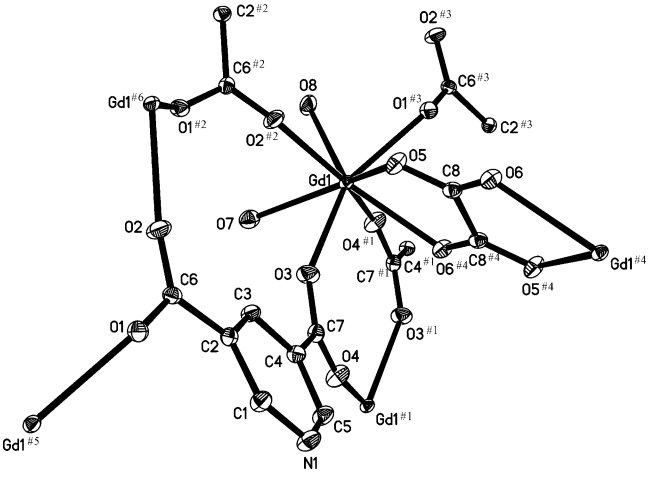

Figure 3. ORTEP drawing of the coordination environments around Lu ions in **2** with thermal ellipsoids at the 40% probability level. The isolated water molecules and H atoms are omitted for clarity.

 © 2008 Wiley-VCH Verlag GmbH & Co. KGaA, Weinheim

[Gd(3,5-pdc)(C_2O_4)$_{0.5}$(H_2O)$_2$]·H_2O (2)

The asymmetric unit of compound **2** contains one Gd^{III} atom, one 3,5-pdc ligand, one-half of an oxalate group, two coordinated water molecules, and one lattice aqua. In **2**, each Gd^{III} atom exhibits a square antiprism geometry, surrounded by eight O atoms, where two come from the coordinated water molecules, two come from one oxalate ligand, and four come from four 3,5-pdc ligands (Figure 3), and the Gd–O bond lengths fall in the range of 2.3095(15) Å to 2.4772(16) Å; these values are comparable to those in the related Gd–carboxylate complexes.[21] Different from **1**, the 3,5-pdc ligand in **2** acts as a μ_4-bridge linking four metal ions through its four carboxylate O atoms, and each metal ion connects four ligands to form a square lattice layer (Figure 4a). The layers are interlinked by oxalate ligands into a porous 3D metal–organic framework, and the lattice water molecules fill the channels along the *b* axis (Figure 4b).

Topological analysis shows that the MOFs consist of 4-connected subunits with a topology of $4^4.6.8$ (Figure 4c). After simplifying the oxalate ligands as links between the metal nodes, the 4-connected subunits are held together by the μ_2-oxalate bridges to generate a novel (4,5)-connected topology (Figure 4d), where the μ_4-bridging pdc ligands act as 4-connected nodes and the metal atoms serve as 5-connected nodes. The topological network can be described by the Schläfli symbol of $(4^4.6.8)(4^4.6^2.8^4)$,[18] the vertex symbol or long symbol of $(4.4.4.4.6.8_8)(4.4.4.4.6.6.8.8.8_9.8_9)$,

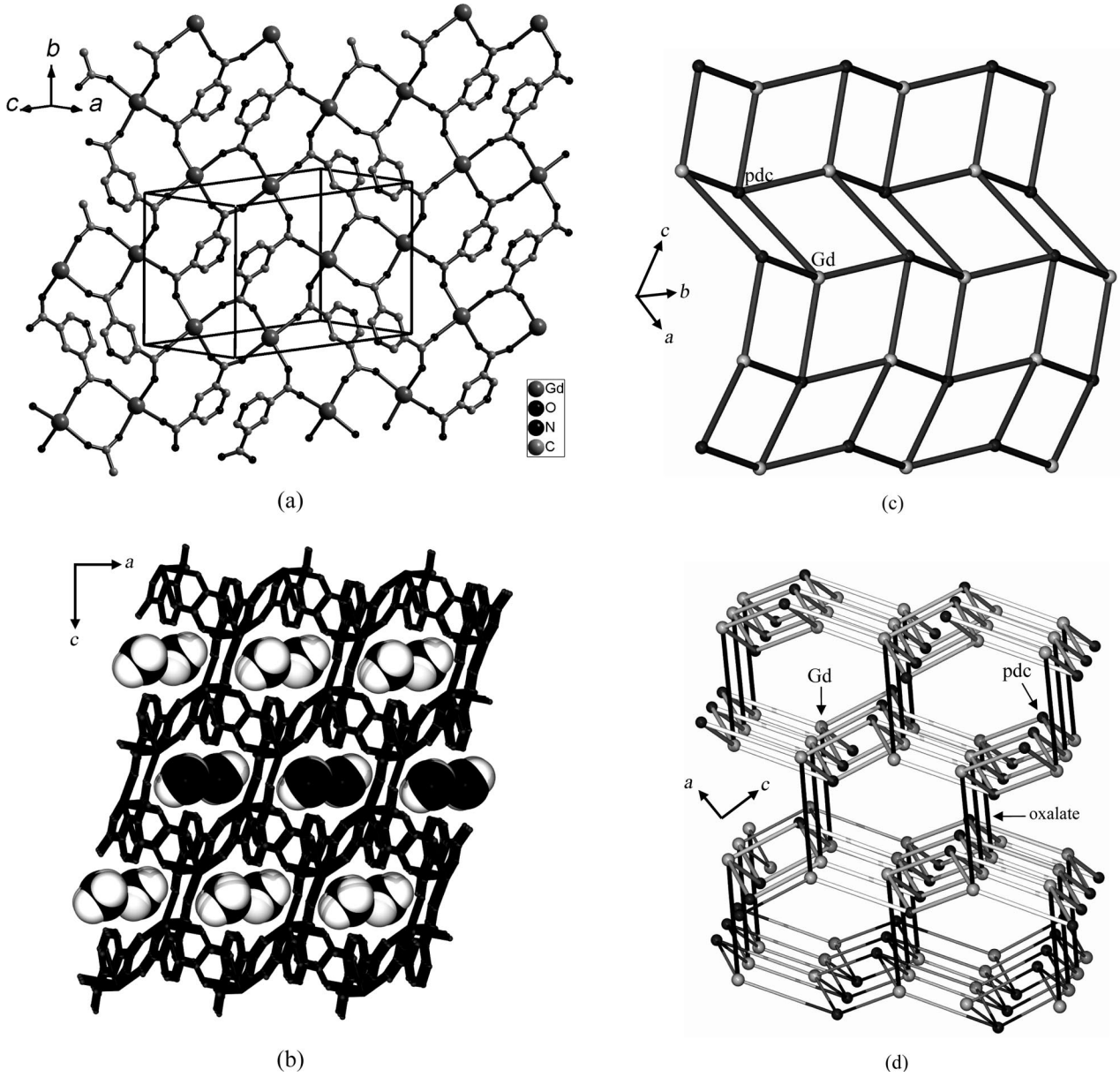

Figure 4. (a) The 2D layer of **2** generated from 3,5-pdc ligands and Gd^{III} atoms; (b) 3D structure of **2**, showing the lattice water molecules occupying the channels along the *b* axis; (c) the 4-connected topological subunit of **2**; (d) the xww topology of **2**, showing 4-connected nodes (black balls) and 5-connected nodes (gray balls) (the black solid lines are oxalate ligands).

 © 2008 Wiley-VCH Verlag GmbH & Co. KGaA, Weinheim

and coordination sequences of (4, 12, 27, 45, 73, 111, 139, 187, 255, 288, 1142) for the 4-connected nodes and (5, 12, 26, 49, 73, 103, 149, 191, 235, 307, 1151) for the 5-connected nodes.[19] This topology represents a novel (4,5)-connected topology that has never been described in the literature. O'Keeffe proposed the $(4^4.6.8)(4^4.6^2.8^4)$-"xww" three-letter code to define the topology. The xww net and the common tcs net have the same layers, but they are differently linked.[12a]

In the crystal structure, the lattice water molecules serve as hydrogen bonds donors, contributing hydrogen atoms to coordinated water O7 and carboxylate O1 atoms, to form O1w–H1A···O7^{i} and O1w–H1B···O1^{ii} hydrogen bonding interactions, respectively [d(O1w···O7^{i}) = 3.152(3) Å, ∠(O1w–H1A···O7^{i}) = 158.59°; d(O1w···O1^{ii}) = 2.827(2) Å, ∠(O1w–H1B···O1^{ii}) = 173.96°; symmetry codes i: –1/2 – x, –1/2 + y, 1/2 – z; ii: –1 + x, –1 + y, z]. The coordinated water molecules (O7) also act as hydrogen donors, donating hydrogen atoms to oxalate O6 atoms and lattice water molecules to form O7–H7A···O6^{iii} and O7–H7B···O1w strong hydrogen bonding interactions, respectively [d(O7···O6^{iii}) = 2.842(2) Å, ∠(O7–H7A···O6^{iii}) = 162.81°; d(O7···O1w) = 2.707(3) Å, ∠(O7–H7B···O1w^{ii}) = 171.35°; symmetry code iii: –1 + x, y, z]. There exists O–H···N strong hydrogen bonding interactions between the uncoordinated pyridyl nitrogen atoms and the coordinated water molecules (O8), by H8B to N1, with d(O8···N1^{iv}) = 0.8539 Å and ∠(O8–H1B···N1^{iv}) = 171.54° (symmetry code iv: –1/2 + x, 5/2 –y, –1/2 + z).

Thermal Stability of Compounds 1 and 2

Thermogravimetric analyses (TGA) for complexes **1** and **2** were measured under a flow of nitrogen gas from room temperature to 600 °C at a heating rate of 10 °C min^{-1}. Complex **1** loses free water molecules and coordinated water molecules in the range 50 °C–280 °C; the observed weight loss of 11.58% is close to the calculated value of 12.33% for release of one free H_2O molecule and two coordinated H_2O molecules per formula unit. Over 370 °C, the sample then further loses weight with increasing temperature. Differential thermal analysis (DTA) shows two strong endothermic reactions at 185 and 460 °C, respectively, which indicates that the framework collapses at 460 °C. For **2**, the first weight loss of 12.60% from 55 to 288 °C corresponds to the loss of two coordinated water molecules and one free water per formula unit (calcd. 12.84%) along with three endothermic peaks at 88, 185, and 274 °C. Upon heating over 360 °C, the sample then begins to further lose weight. DTA curves display that one strong exothermic reaction occurs at 403 °C because of the collapse of the framework of **2**.

Fluorescence Properties

The solid-state fluorescent spectra of **1**–**4** at room temperature are depicted in Figure 5. All the complexes exhibit stronger fluorescence compared to that of the free ligands (a weak emission at ca. 415 nm in the solid state). When excited at 370 nm at room temperature, **1** emits a strong luminescence with the maximum wavelength centered at 430 nm, which would likely originate from intraligand $\pi_L \rightarrow \pi_L^*$ transition emissions (LLCT). Different from **1**, compound **2** shows significant strong-green luminescence with a broad emission maximum peak centered at ca. 510 nm and a relatively weak luminescence with the emission maximum peak at ca. 400 nm upon excitation at λ = 340 nm. Complexes **3** and **4**, displaying similar photoluminescent properties, emit significant strong-green luminescence with a broad emission maximum peak centered at ca. 500 nm and a strong luminescence with the emission maximum peak at ca. 420 nm. The strong-green luminescent emission of complexes **2**–**4** would be assigned to the ligand-to-metal charge transfer (LMCT) and/or metal-to-ligand charge transfer (MLCT). The luminescent emission at ca. 410 nm would be attributed to intraligand $\pi_L \rightarrow \pi_L^*$ transitions emission (LLCT). The fluorescence enhancement of **1**–**4** may be due to the coordination interactions and 3D framework structures, which effectively increase the rigidity of the ligand and reduce the loss of energy by radiationless decay of the intraligand emission excited state.[22] Thus, complex **1** may be used for blue-fluorescent materials and **2**–**4** may be suitable as a candidate of green-fluorescent materials.

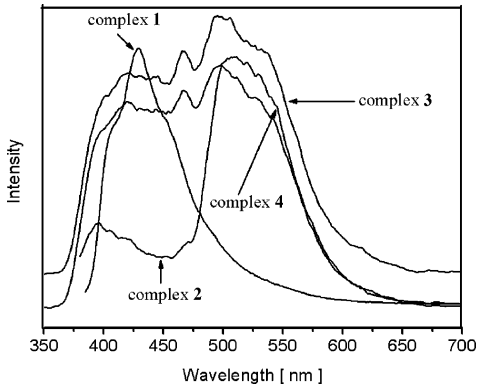

Figure 5. The photoluminescent emission spectra for **1**–**4** in the solid state at room temperature.

Conclusions

Four rare topological net MOFs were prepared by hydrothermal reactions of 3,5-H_2pdc with lanthanide oxide and perchloric acid. Compound **1** shows uncommon (3,4)-connected $(4.8^2)(4.8^5)$ dmc-type topological network, and complexes **2**–**4** display a novel (4,5)-connected $(4^4.6.8)(4^4.6^2.8^4)$-"xww" topology. Furthermore, this contribution confirms the feasibility of the lanthanide-mediated in situ transformation of CO_2 to oxalate under hydrothermal conditions. The results are not only important for the understanding of the in situ CO_2 coupling mechanism under hydrothermal conditions, but they also afford valuable information for the generation of photoluminescent materials and contribute to the discovery of new and previously unrecognized topologies.

 © 2008 Wiley-VCH Verlag GmbH & Co. KGaA, Weinheim

Experimental Section

General: All chemicals of reagent grade were commercially available and used without further purification. Elemental analysis was performed with a Perkin–Elmer 2400 CHNS/O analyzer. The infrared spectrum of KBr pellets in the range 4000–400 cm^{-1} was recorded with a Nicolet AVATAR-370 spectrophotometer. Thermogravimetric analyses (TGA) were carried out with a NETZSCH STA449C instrument. Fluorescent properties of **1**–**4** were measured with an Edinburgh Instruments analyzer model FL920. X-ray powder diffraction was performed with an X′Pert PRODY2198 diffractometer with Cu-K_α radiation (λ = 1.5418 Å).

[Lu(3,5-pdc)$(C_2O_4)_{0.5}(H_2O)_2$]·H_2O (1): The hydrothermal reaction of 3,5-pdc, Lu_2O_3, perchloric acid and water in a molar ratio 1:1:4:500 at 200 °C for 2 d, then at 190 °C for 3 d, afforded beige crystals of **1**. Yield: 0.11 g (25%). IR (KBr): $\tilde{\nu}$ = 3399 (m), 1687 (s), 1604 (s), 1545 (s), 1442 (s), 1405 (s), 1317 (m), 1124 (w), 1031 (w), 941 (w), 837 (m), 806 (m), 771 (m), 692 (m), 531 (w) cm^{-1}. $C_8H_9LuNO_9$ (438.13): calcd. C 21.91, H 2.05, N 3.20; found C 21.85, H 2.09, N 3.18.

[Gd(3,5-pdc)$(C_2O_4)_{0.5}(H_2O)_2$]·H_2O (2): This complex was prepared as above by using Gd_2O_3 instead of Lu_2O_3. Yield: 0.10 g (23%). IR (KBr): $\tilde{\nu}$ = 3440 (s), 3142 (m), 1692 (s), 1604 (s), 1537 (s), 1465 (s), 1407 (s), 1371 (m), 1150 (w), 849 (w), 806 (m), 765 (m), 723 (m), 698 (m), 610 (w), 536 (m) cm^{-1}. $C_8H_9GdNO_9$ (420.41): calcd. C 22.83, H 2.14, N 3.33; found C 22.85, H 2.10, N 3.32.

[Tm(3,5-pdc)$(C_2O_4)_{0.5}(H_2O)_2$]·H_2O (3): This complex was prepared as above by using Tm_2O_3 instead of Lu_2O_3. Yield: 0.09 g (20%). IR (KBr): $\tilde{\nu}$ = 3546 (m), 3440 (m), 3317 (m), 3087 (m), 1682 (m), 1606 (s), 1560 (s), 1439 (m), 1393 (s), 1321 (m), 1151 (w), 804 (m), 769 (m), 719 (m), 612 (w), 538 (w) cm^{-1}. $C_8H_9NO_9Tm$ (432.09): calcd. C 22.22, H 2.08, N 3.24; found C 22.27, H 2.13, N 3.28.

[Yb(3,5-pdc)$(C_2O_4)_{0.5}(H_2O)_2$]·H_2O (4): This complex was prepared as above by using Yb_2O_3 instead of Lu_2O_3. Yield: 0.09 g (20%). IR (KBr): $\tilde{\nu}$ = 3547 (m), 3444 (m), 3317 (m), 1687 (m), 1605 (s), 1565 (s), 1439 (m), 1395 (s), 1322 (m), 1150 (w), 804 (w), 768 (w), 721 (m), 612 (w), 538 (m) cm^{-1}. $C_8H_9NO_9Yb$ (435.19): calcd. C 22.01, H 2.06, N 3.21; found C 22.05, H 2.10, N 3.26.

[Ln(3,5-pdc)$(C_2O_4)_{0.5}(H_2O)_2$]·H_2O: (Ln = Dy^{III}, Sm^{III}, Ho^{III}, Eu^{III}, La^{III}, Nd^{III}, and Er^{III} for complex **5**–**11**, respectively): These complexes was prepared as above only by using different lanthanide oxides with yields ca. 20% (based on the initial Ln_2O_3 input).

X-ray Crystallography: Single crystals of complexes **1**–**4** with dimensions $0.32 \times 0.28 \times 0.26$ (**1**), $0.22 \times 0.18 \times 0.16$ (**2**), $0.38 \times 0.35 \times 0.29$ (**3**), and $0.33 \times 0.31 \times 0.29$ mm (**4**) were mounted on glass fibers for their respective crystal structure analysis. Data collection for **1**–**4** were performed with a Bruker SMART-CCD diffractometer equipped with a graphite monochromated Mo-K_α radiation (λ = 0.71073 Å) at 293 K. The structures were solved by direct methods, the metal atoms were located from the E-maps, and other non-hydrogen atoms were derived from the successive difference Fourier Syntheses. The hydrogen atoms were located from the difference map and refined isotropically. The structures were refined by full-matrix, least-squares minimizations of $\Sigma(F_o - F_c)^2$ with anisotropic thermal parameters for all non-hydrogen atoms and all calculations were performed by using the SHELXTL-97 program package.[23] Complexes **5**–**7** are confirmed by X-ray single crystal structural diffraction analyses, and **8**–**11** are only confirmed by the lattice parameters by the X-ray single crystal structural diffraction analyses. Table 3 summarizes the important crystal data for **1**–**4**.

The experimental XRD patterns (Supporting Information) agreed well with the simulated ones generated on the basis of single-crystal analyses of **1**–**4**, suggesting the phase purity of the products.

CCDC-649010, -649011, -649012, and -649013 for **1**–**4** contain the supplementary crystallographic data for this paper. These data can be obtained free of charge from The Cambridge Crystallographic Data Centre via www.ccdc.cam.ac.uk/data_request/cif.

Table 3. Crystal data summary for **1**–**4**.

	1	**2**	**3**	**4**
Formula	$C_8H_9LuNO_9$	$C_8H_9GdNO_9$	$C_8H_9TmNO_9$	$C_8H_9YbNO_9$
Formula weight	438.13	420.41	432.09	435.19
Description	block	block	block	block
Temperature [K]	293(2)	293(2)	293(2)	293(2)
Crystal system	Monoclinic	Monoclinic	Monoclinic	Monoclinic
Space group	$P2_1/c$	$P2_1/n$	$P2_1/n$	$P2_1/n$
a [Å]	13.310(3)	7.6435(15)	7.5716(7)	7.6026(10)
b [Å]	12.825(3)	9.840(2)	9.7891(9)	9.7798(13)
c [Å]	6.6008(13)	14.785(3)	14.6702(13)	14.6423(19)
β [°]	103.63(3)	98.27(3)	97.9330(10)	98.075(2)
Volume [$Å^3$]	1095.0(4)	1100.5(4)	1076.94(17)	1077.9(2)
Z	4	4	4	4
$D_{calcd.}$ [$g\,cm^{-3}$]	2.658	2.537	2.665	2.682
F(000)	828	800	820	820
μ [mm^{-1}]	9.063	6.073	8.286	8.724
θ Range [°]	3.15–27.47	3.20–27.47	2.51–28.38	2.51–28.29
Size [mm]	$0.32 \times 0.28 \times 0.26$	$0.22 \times 0.18 \times 0.16$	$0.38 \times 0.35 \times 0.29$	$0.33 \times 0.31 \times 0.29$
Total data	10587	10554	9732	9685
Unique data	2509	2516	2681	2642
Parameters	173	173	196	172
R_{int}	0.0333	0.0189	0.0712	0.1175
$R_1[I > 2\sigma(I)]$[a]	0.0210	0.0138	0.0200	0.0314
$wR_2[I > 2\sigma(I)]$[b]	0.0584	0.0285	0.0402	0.0733
R_1(all data)	0.0234	0.0153	0.0243	0.0347
wR_2(all data)	0.0746	0.0288	0.0414	0.0748
GOF (S)	1.294	1.155	1.007	1.039

[a] $R_1 = \Sigma(|F_o| - |F_c|)/\Sigma|F_o|$. [b] $wR_2 = [\Sigma w(F_o^2 - F_c^2)^2/\Sigma w(F_o^2)^2]^{1/2}$.

 © 2008 Wiley-VCH Verlag GmbH & Co. KGaA, Weinheim

Abbreviations for 3D nets have been taken from *Reticular Chemistry Structure Resource*,[24] and the vertex symbol calculation was used *TOPOS4*.[25]

Supporting Information (see footnote on the first page of this article): The simulated and experimental PXRD patterns of compounds **1**–**4**.

Acknowledgments

This work are supported by the Natural Science Foundation of China (NSFC, 60508012). G. Z. is supported by the fund for Distinguished Young Scholars of Hubei Province of China under grant No. 2006ABB031. X. L. is supported by the Scientific Research Fund of Ningbo University.

[1] a) S. R. Batten, R. Robson, *Angew. Chem. Int. Ed.* **1998**, *37*, 1460–1494; b) M. Eddaoudi, D. B. Moler, H. Li, B. Chen, T. M. Reineke, M. O'Keeffe, O. M. Yaghi, *Acc. Chem. Res.* **2001**, *34*, 319–330; c) G. S. Papaefstathiou, L. R. MacGillivray, *Coord. Chem. Rev.* **2003**, *246*, 169–184; d) O. R. Evans, W. Lin, *Acc. Chem. Res.* **2002**, *35*, 511–522; e) B. Moulton, M. J. Zaworotko, *Chem. Rev.* **2001**, *101*, 1629–1658; f) S. Kitagawa, R. Kitaura, S. Noro, *Angew. Chem. Int. Ed.* **2004**, *43*, 2334–2375; g) C. N. R. Rao, S. Natarajan, R. Vaidhyanathan, *Angew. Chem. Int. Ed.* **2004**, *43*, 1466–1496.

[2] a) J. S. Seo, D. Whang, H. Lee, S. I. Jun, J. Oh, Y. J. Jeon, K. Kim, *Nature* **2000**, *404*, 982–986; b) O. R. Evans, H. L. Ngo, W. Lin, *J. Am. Chem. Soc.* **2001**, *123*, 10395–10396; c) W. Lin, *J. Solid State Chem.* **2005**, *178*, 2486–2490.

[3] a) H. Li, M. Eddaoudi, M. O'Keeffe, O. M. Yaghi, *Nature* **1999**, *402*, 276–279; b) M. Eddaoudi, J. Kim, N. Rosi, D. Vodak, J. Wachter, M. O'Keeffe, O. M. Yaghi, *Science* **2002**, *295*, 469–472; c) J. L. C. Rowsell, E. C. Spencer, J. Eckert, J. A. K. Howard, O. M. Yaghi, *Science* **2005**, *309*, 1350–1354; d) G. Férey, C. Mellot-Draznieks, C. Serre, F. Millange, J. Dutour, S. Surblé, I. Margiolaki, *Science* **2005**, *309*, 2040–2042.

[4] a) A. J. Tasiopoulos, A. Vinslava, W. Wernsdorfer, K. A. Abboud, G. Christou, *Angew. Chem. Int. Ed.* **2004**, *43*, 2117–2121; b) M. Murugesu, M. Habrych, W. Wernsdorfer, K. A. Abboud, G. Christou, *J. Am. Chem. Soc.* **2004**, *126*, 4766–4767; c) G. J. Halder, C. J. Kepert, B. Moubaraki, K. S. Murray, J. D. Cashion, *Science* **2002**, *298*, 1762–1765.

[5] G. B. Deacon, R. Philips, *Coord. Chem. Rev.* **1980**, *88*, 227–250.

[6] a) H. K. Chae, M. Eddaoudi, J. Kim, S. I. Hauck, J. F. Hartwig, M. O'Keeffe, O. M. Yaghi, *J. Am. Chem. Soc.* **2001**, *123*, 11482–11483; b) J. L. C. Rowsell, A. R. Millward, K. S. Park, O. M. Yaghi, *J. Am. Chem. Soc.* **2004**, *126*, 5666–5667; c) J. L. C. Rowsell, O. M. Yaghi, *J. Am. Chem. Soc.* **2006**, *128*, 1304–1315; d) M. Eddaoudi, J. Kim, N. Rosi, D. Vodak, J. Wachter, M. O'Keeffe, O. M. Yaghi, *Science* **2002**, *298*, 469–472; e) J. L. C. Rowsell, E. C. Spencer, J. Eckert, J. A. K. Howard, O. M. Yaghi, *Science* **2005**, *309*, 1350–1354; f) N. L. Rosi, J. Kim, M. Eddaoudi, B. Chen, M. O'Keeffe, O. M. Yaghi, *J. Am. Chem. Soc.* **2005**, *127*, 1504–1518.

[7] a) L.-Y. Zhang, G.-F. Liu, S.-L. Zheng, B.-H. Ye, X.-M. Zhang, X.-M. Chen, *Eur. J. Inorg. Chem.* **2003**, 2965–2971; b) J. Tao, M.-L. Tong, J.-X. Shi, X.-M. Chen, S. W. Ng, *Chem. Commun.* **2000**, 2043–2044; c) C. S. McCowan, T. L. Groy, M. T. Caudle, *Inorg. Chem.* **2002**, *41*, 1120–1127; d) E. Y. Lee, S. Y. Jang, M. P. Suh, *J. Am. Chem. Soc.* **2005**, *127*, 6374–6381; e) K. Hanson, N. Calin, D. Bugaris, M. Scancella, S. C. Sevov, *J. Am. Chem. Soc.* **2004**, *126*, 10502–10503; f) R. C. Mehrotra, R. Bohra, *Metal Carboxylates*, Academic, New York, **1983**.

[8] a) L. Öhrström, K. Larsson, *Molecule-Based Materials*: *The Structural Network Approach*, Elsevier, Amsterdam, **2005**; b) N. W. Ockwig, O. Delgado-Friedrichs, M. O'Keeffe, O. M. Yaghi, *Acc. Chem. Res.* **2005**, *38*, 176–182; c) I. A. Baburin, V. A. Blatov, L. Carlucci, G. Ciani, D. M. Proserpio, *J. Solid State Chem.* **2005**, *178*, 2452–2474; d) V. A. Blatov, L. Carlucci, G. Ciani, D. M. Proserpio, *CrystEngComm* **2004**, *6*, 377–395.

[9] A. F. Wells, *Three-Dimensional Nets and Polyhedra*, Wiley-Interscience, New York, **1977**.

[10] M. A. M. Abu-Youssef, V. Langerb, L. Öhrström, *Chem. Commun.* **2006**, 1082–1084.

[11] J. A. Rodgers, W. T. A. Harrison, *Chem. Commun.* **2000**, 2385–2386.

[12] a) W. B. Pearson, *J. Solid State Chem.* **1985**, *56*, 278–287; b) S. R. Batten, *CrystEngComm* **2001**, *3*, 67–73.

[13] a) J. Ballato, J. S. Lewis, P. Holloway, *Mater. Res. Soc. Bull.* **1999**, *24*, 51–56; b) A. J. Steckl, J. M. Zavada, *Mater. Res. Soc. Bull.* **1999**, *24*, 33–38; c) M. Bredol, U. Kynast, C. Ronda, *Adv. Mater.* **1991**, *3*, 361–367.

[14] a) Y.-Q. Sun, J. Zhang, Y.-M. Chen, G.-Y. Yang, *Angew. Chem. Int. Ed.* **2005**, *44*, 5814–5817; b) M. R. Bnrgstein, M. T. Gamer, P. W. Roesky, *J. Am. Chem. Soc.* **2004**, *126*, 5213–5218; c) T. M. Reineke, M. Eddaoudi, M. O'Keeffe, O. M. Yaghi, *Angew. Chem. Int. Ed.* **1999**, *38*, 2590–2594; d) D.-L. Long, A. J. Blake, N. R. Champness, C. Wilson, M. Schröder, *J. Am. Chem. Soc.* **2001**, *123*, 3401–3402.

[15] a) M. M. Halmann, *Chemical Fixation of Carbon Dioxide*, CRC Press, Boca Raton, **1993**; b) F. Hutschka, A. Dedieu, M. Eichberger, R. Fornika, W. Leitner, *J. Am. Chem. Soc.* **1997**, *119*, 4432–4443; c) N. Komeda, H. Nagao, T. Matsui, G. Adachi, K. Tanaka, *J. Am. Chem. Soc.* **1992**, *114*, 3625–3630; d) J. Fischer, Th. Lehmann, E. Heitz, *J. Appl. Electrochem.* **1981**, *11*, 743–750; e) X. Li, R. Cao, D. Sun, Q. Shi, W. Bi, M. Hong, *Inorg. Chem. Commun.* **2003**, *6*, 815–818; f) D. Min, S. W. Lee, *Inorg. Chem. Commun.* **2002**, *5*, 978–983; g) H. S. Huh, S. W. Lee, *Bull. Korean Chem. Soc.* **2006**, *27*, 1839–1843; h) W. J. Evans, C. A. Seibel, J. W. Ziller, *Inorg. Chem.* **1998**, *37*, 770–776; i) J. Y. Lu, A. M. Babb, *Inorg. Chem.* **2002**, *41*, 1339–1341.

[16] a) Q.-Y. Liu, L. Xu, *Eur. J. Inorg. Chem.* **2005**, 3458–3466; b) H.-L. Sun, C.-H. Ye, X.-Y. Wang, J.-R. Li, S. Gao, K.-B. Yu, *J. Mol. Struct.* **2004**, *702*, 77–83.

[17] A. F. Wells, *Acta Crystallogr., Sect. A* **1986**, *42*, 133–134.

[18] J. V. Smith, *Am. Mineral.* **1978**, *63*, 960–969.

[19] a) M. O'Keeffe, B. G. Hyde, *Crystal Structures I: Patterns and Symmetry, Mineralogical Society of America*, Washington, **1996**; b) O. Delgado-Friedrichs, M. O'Keeffe, *J. Solid State Chem.* **2005**, *178*, 2480–2485.

[20] a) O. D. Friedrichs, M. O'Keeffe, O. M. Yaghi, *Acta Crystallogr., Sect. A* **2003**, *59*, 22–27; b) O. D. Friedrichs, M. O'Keeffe, *Acta Crystallogr., Sect. A* **2005**, *61*, 358–362; c) O. D. Friedrichs, M. O'Keeffe, O. M. Yaghi, *Acta Crystallogr., Sect. A* **2006**, *62*, 350–355.

[21] a) Y. Cui, H. L. Ngo, P. S. White, W. Lin, *Chem. Commun.* **2002**, 1666–1667; b) T. K. Maji, G. Mostafa, H.-C. Chang, S. Kitagawa, *Chem. Commun.* **2005**, 2436–2438; c) C. Qin, X.-L. Wang, E.-B. Wang, Z.-M. Su, *Inorg. Chem.* **2005**, *44*, 7122–7129.

[22] Yersin, H.; Vogler, A. *Photochemistry and Photophysics of Coordination Compounds*, Springer, Berlin, **1987**.

[23] G. M. Sheldrick, *SHELXL–97: Programm zur Verfeinerung von Kristallstrukturen*, Göttingen, **1997**.

[24] M. O'Keeffe, O. M. Yaghi, *Reticular Chemistry Structure Resource*, Arizona State University, Tempe, **2005**, http://okeeffe-ws1.la.asu.edu/rcsr/home.htm.

[25] a) V. A. Blatov, **2006**, http://www.topos.ssu.samara.ru/; b) V. A. Blatov, A. P. Shevchenko, V. N. Serezhkin, *J. Appl. Crystallogr.* **2000**, *33*, 1193.

Received: August 1, 2007
Published Online: November 7, 2007

 © 2008 Wiley-VCH Verlag GmbH & Co. KGaA, Weinheim